Available online at www.sciencedirect.com
ScienceDirect
Biochimica et Biophysica Acta 1778 (2008) 521–529
Biochimica et Biophysica Acta
BBA
www.elsevier.com/locate/bbamem

Subunit-selective role of the M3 transmembrane domain of the nicotinic acetylcholine receptor in channel gating

María José De Rosa, Jeremías Corradi, Cecilia Bouzat *

Instituto de Investigaciones Bioquímicas, Universidad Nacional del Sur-CONICET, Camino La Carrindanga Km 7, B8000FWB, Bahía Blanca, Argentina

Received 19 June 2007; received in revised form 25 September 2007; accepted 29 October 2007
Available online 4 November 2007

Abstract

The nicotinic acetylcholine receptor (AChR) can be either hetero-pentameric, composed of α and non-α subunits, or homo-pentameric, composed of α7 subunits. To explore the subunit-selective contributions of transmembrane domains to channel gating we analyzed single-channel activity of chimeric muscle AChRs. We exchanged M3 between α1 and ε or α7 subunits. The replacement of M3 in α1 by εM3 significantly alters activation properties. Channel activity appears as bursts of openings whose durations are 20-fold longer than those of wild-type AChRs. In contrast, 7-fold briefer openings are observed in AChRs containing the reverse ε chimeric subunit. The duration of the open state decreases with the increase in the number of α1M3 segments, indicating additive contributions of M3 of all subunits to channel closing. Each α1M3 segment decreases the energy barrier of the closing process by ~0.8 kcal/mol. Partial chimeric subunits show that small stretches of the M3 segment contribute additively to the open duration. The replacement of α1 sequence by α7 in M3 leads to 3-fold briefer openings whereas in M1 it leads to 10-fold prolonged openings, revealing that the subunit-selective role is unique to each transmembrane segment.

Keywords: Nicotinic receptor; Single-channel; Patch-clamp; Transmembrane domains

1. Introduction

The nicotinic acetylcholine receptor (AChR), member of the Cys-loop receptor superfamily, is of fundamental importance in the synaptic transmission at the neuromuscular junction and throughout the nervous system. AChR subunits are classified as α, which contain a disulphide bridge involved in the recognition and binding of agonists, and non-α subunits, which lack this motif. The primordial AChR presumably contained only one type of α subunit and evolution led to subunit diversity resulting in a wide spectrum of structurally and functionally different AChRs [1]. The AChR has a composition of $(\alpha1)_2\beta\delta\gamma$ in fetal and $(\alpha1)_2\beta\delta\varepsilon$ in adult muscle. In brain, receptors are made up either of different combinations of α (α2−α10) and β subunits (β2−β7) or of five identical α subunits, such as the neuronal α7 subtype. Each AChR subtype exhibits unique pharmacology and ion channel properties. Little is known about the selective role of each subunit during AChR activation.

AChR subunits share a similar structure: an amino-terminal extracellular domain, which includes the ACh binding sites, and a transmembrane region composed of four transmembrane segments (M1–M4). All four segments have been shown to contribute to channel function. The M2 domain delineates the ion pore, contributes to the cation selectivity and moves to allow ion flux [2–7]. The M1 domain appears to be involved in agonist dissociation and channel gating [8,9]. The M4 domain moves during channel activation and it may modulate AChR kinetics through its contacts with membrane lipids [10–14]. M3 also contributes to channel gating [15–17]. By tryptophan-scanning mutagenesis it has been postulated that M3 undergoes a spring motion during ion channel activation [18]. More recently, it was determined that M3 moves after M2 and M4 domains during the channel-opening process [19].

To further understand the role of the M3 transmembrane segment in each subunit of the pentameric receptor during channel activation we constructed chimeric subunits. We exchanged M3 between α and non-α subunits and between subunits that form homo- and hetero-pentameric receptors. To determine if the consequences of the transmembrane segment swapping are

* Corresponding author. Fax: +54 291 4861200.
E-mail address: inbouzat@criba.edu.ar (C. Bouzat).

0005-2736/$ - see front matter © 2007 Elsevier B.V. All rights reserved.
doi:10.1016/j.bbamem.2007.10.026

similar for different domains, we swapped α1M1 with M1 of ε and α7. Our results provide new evidence for the subunit-selective roles of M1 and M3 transmembrane domains and help to understand the differential contribution of subunits to channel activation.

2. Materials and methods

2.1. Construction of mutant and chimeric subunits and AChR expression

Chimeric and mutant subunits were constructed using the QuikChange™ Site-Directed mutagenesis kit (Strategene, Inc., TX). Restriction mapping and DNA sequencing confirmed all constructs.

HEK293 cells were transfected with mouse α1, β, δ, and ε cDNA subunits (wild-type or mutant) using calcium phosphate precipitation, essentially as described previously [20,21]. Cells were used for single-channel measurements 1 or 2 days after transfection. Surface expression of M3 chimeras was measured by determing the total number of [^{125}I]α-BTX binding sites. Transfected cells were incubated 2 h with 5 nM [^{125}I]α-BTX at room temperature. Non-specific binding was determined in the presence of 20 mM carbamylcholine. The total number of binding sites for all chimeric receptors varied between 3 and 10% of that of wild-type AChRs.

2.2. Patch-clamp recordings

Recordings were obtained in the cell-attached configuration [22] at a membrane potential of −70 mV and at 20 °C. The bath and pipette solutions contained 142 mM KCl, 5.4 mM NaCl, 1.8 mM $CaCl_2$, 1.7 mM $MgCl_2$ and 10 mM HEPES (pH 7.4). Single-channel currents were recorded using an Axopatch 200 B patch-clamp amplifier (Molecular Devices Corporation), digitized at 5 μs intervals with the PCI-6111E interface (National Instruments, Austin, TX), and detected by the half-amplitude threshold criterion using the program TAC 4.0.10 (Bruxton Corporation) at a final bandwidth of 10 kHz [13]. Open- and closed-time histograms were fitted to the sum of exponential functions by maximum likelihood using the program TACFit (Bruxton Corporation).

Kinetic analysis was performed as described before [8,12,13]. The analysis was restricted to clusters of channel openings, each reflecting the activity of a single AChR. Clusters of openings corresponding to a single AChR were identified as a series of closely spaced events preceded and followed by closed intervals longer than a critical duration (τ_{crit}). This duration was taken as the point of intersection of the predominant closed component and the succeeding one in the closed-time histogram. The predominant closed duration component, which becomes shorter with the increase of agonist concentration, reflects the set of transitions between unliganded closed and diliganded open states. To minimize errors in assigning cluster boundaries, we analyzed only recordings from patches with low channel activity. Only clusters containing more than 10 openings and not showing double openings were considered for further analysis. For each recording, kinetic homogeneity was determined by selecting clusters on the basis of their distribution of mean open duration, mean closed duration and open probability [8,12,13]. Typically, more than 80% of the clusters were selected, and between 2000 and 10,000 events of each condition were used for the analysis. The resulting open and closed intervals from single patches at several ACh concentrations were analyzed according to kinetic schemes using QUB Software (QuB Suite, State University of New York, Buffalo). The dead time was typically 30 μs. Probability density functions of open and closed durations were calculated from the fitted rate constants and instrumentation dead time and superimposed on the experimental dwell time histogram as described by Qin et al. [23]. Calculated rates were accepted only if the resulting probability density functions correctly fitted the experimental open and closed duration histograms. Standard errors of the rate constants estimates were calculated by the program from the curvature of the likelihood surface at its maximum [23,24]. For wild-type AChRs the opening rate of the diliganded AChR, β_2 in Scheme 1, was constrained to its previously determined value [8,25,26] because brief closings due to gating and channel blocking become indistinguishable at high ACh concentrations [8,12,26]. Also, the association and dissociation rate constants were assumed to be equal at both binding sites [8,26,27].

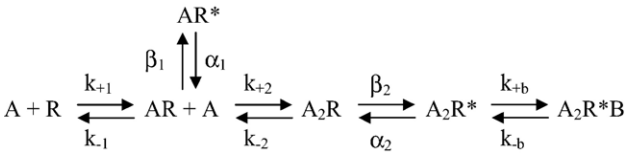

Scheme 1.

Energy changes between different AChRs in channel closing were estimated as:

$$\Delta(\Delta Gc) = -RT \ln [(1/\text{mutant mean open time})/(1/\text{wild-type mean open time})] \quad (1)$$

where R is the gas constant and T is the absolute temperature. The closing rate was estimated by 1/mean open time. Open probability within clusters (P_{open}) was determined experimentally at each ACh concentration by calculating the mean fraction of time that the channel is open within a cluster.

For outside-out patch recordings, the pipette solution contained 134 mM KCl, 5 mM EGTA, 1 mM $MgCl_2$, and 10 mM HEPES (pH 7.3). Bath solution contained 150 mM NaCl, 1.8 mM $CaCl_2$, 1 mM $MgCl_2$, and 10 mM HEPES (pH 7.3). A series of applications of bath solution containing 1 mM ACh were applied to the patch as described before [28,29]. Macroscopic currents were filtered at 5 kHz. Data analysis was performed using the IgorPro software (WaveMetrics Inc., Lake Oswego, Oregon). The ensemble mean current was calculated for 5–10 individual current traces. Mean currents were fitted by a single exponential function:

$$I_{(t)} = I_0 \exp(-t/\tau_d) + I_\infty \quad (2)$$

where I_0 and I_∞ are the peak and the steady state current values, respectively, and τ_d is the decay time constant that measures the current decay due to desensitization.

3. Results

3.1. M3 chimeric subunits assemble into functional receptors

To determine the specific role of the M3 segment of each subunit we constructed a series of chimeric receptors. We exchanged M3 between muscle α1 and ε subunits, and between α subunits forming hetero-(α1) or homo-oligomers (α7). We expressed the chimeric subunits with the complement wild-type subunits. Macroscopic currents recorded from outside-out patches rapidly perfused with 1 mM ACh reveal that the chimeric subunits are incorporated into functional receptors (Fig. 1). Currents are smaller than wild-type currents, probably due to the reduced cell surface expression, which is lower than 10% of that of wild-type AChR in all chimeric receptors (see Materials and methods). In contrast, the current decay time constants (τ_d) are similar to that of wild-type AChRs (τ_d=25±8 ms, 22±6, 27±7 and 25±3 ms for wild-type, α1(M3ε), ε(M3α1) and α1(M3α7), respectively).

Co-transfection of cells with chimeric and wild-type cDNA subunits could result in the surface expression of chimeric subunit-omitted AChRs. We can ensure that the chimeric subunits are incorporated into functional receptors because the absence of α1 cannot lead to functional receptors, and because channel activity recorded from cells transfected with α1, β, δ and the chimeric ε subunit is quite different to that of ε-lacking AChRs ($\alpha 1_2\beta\delta_2$) [20]. Considering the following issues, it is probable

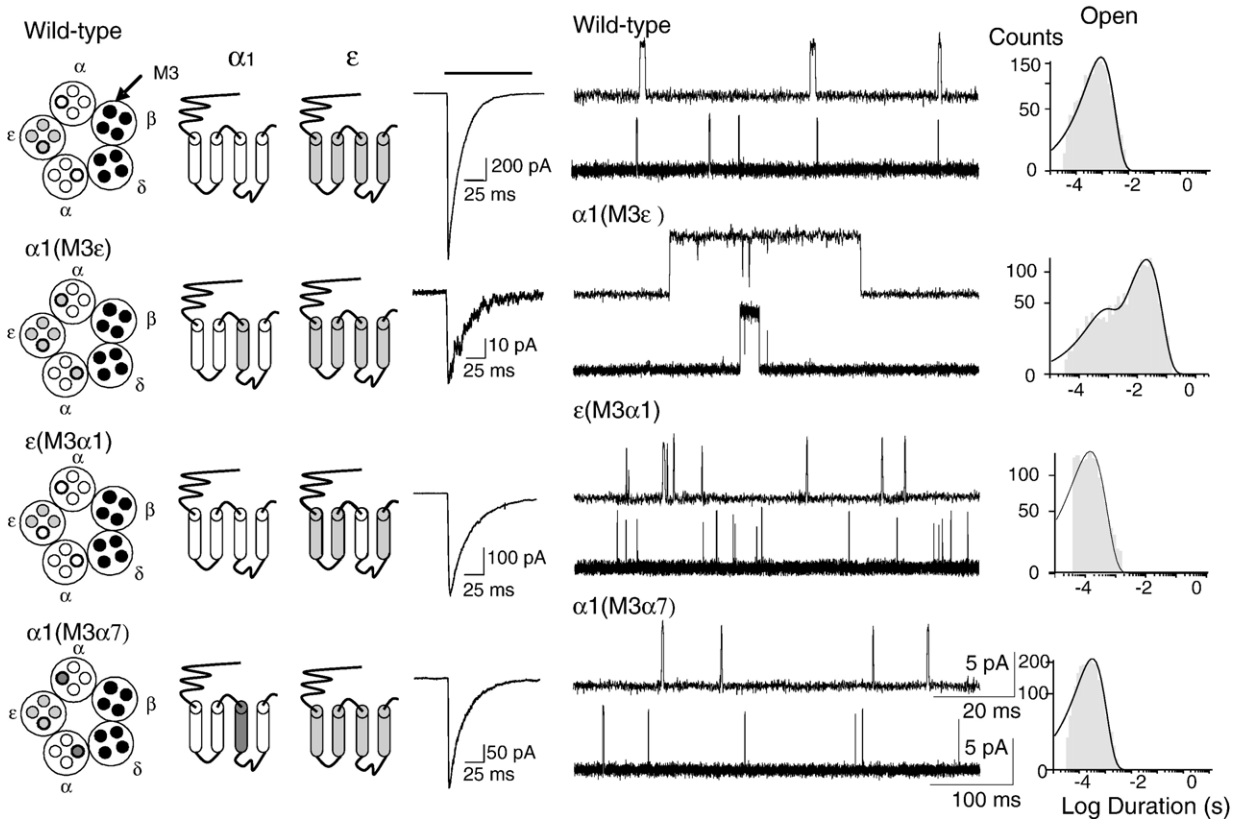

Fig. 1. Macroscopic and single-channel currents of wild-type and M3 chimeric AChRs. *Left*. Subunit arrangement of wild-type and M3 chimeric AChRs and schematic diagram of the transmembrane region of α1 and ε subunits. Segments in white correspond to α1, in light grey to ε, in dark grey to α7, and in black to β and δ subunits. *Middle*. Currents recorded from outside-out patches in response to rapid application of 1 mM ACh. The solid bar indicates the duration of the exposure to agonist. Each trace represents the average of 6–10 applications of agonist. Membrane potential: −50 mV. *Right*. Single-channels activated by 1 μM ACh. Currents are displayed at a bandwidth of 9 kHz with channel openings as upward deflections. Membrane potential: −70 mV. Open-time histograms for AChRs carrying the specified chimeric subunit are shown. The mean durations and relative areas of the open components in the histograms are: wild-type=0.96 ms (0.85) and 0.21 ms; α1(M3ε)=23.50 ms (0.70) and 0.53 ms; ε(M3α1)=0.16 ms (1); α1(M3α7)=0.27 ms (1).

that the arrangement of the subunits in the pentameric receptors remains as in wild-type AChRs. Firstly, the muscle AChR shows a tightly constrained structure with a fixed anti-clockwise α1εα1δβ order of subunits, which is essential for channel activation and specific and precise contributions from α and non-α subunits are required for agonist binding and channel gating [5,30]. Secondly, assembly of AChR is a tightly regulated and ordered process, which requires appropriate subunit–subunit interactions, mainly mediated by the extracellular domain of AChR subunits [31–34].

3.2. Channel properties are significantly altered in M3 chimeric AChRs

To determine the functional consequences of exchanging the M3 segment between subunits we analyzed single-channels activated by 1 μM ACh (Fig. 1). At this low ACh concentration, wild-type channels appear mainly as isolated channels or as bursts of 2 openings ([35] and Fig. 1). The replacement of M3 in α1 by that of the ε subunit (α1(M3ε) chimera) significantly alters activation properties. Channel activity appears as single brief openings together with bursts of longer openings, each containing an average number of 4 opening events and a mean duration of 74±5 ms. The open-time histogram shows a main component of about 20 ms, which corresponds mainly to openings within bursts, and a minor component of 0.57±0.20 ms, which corresponds to isolated openings (Fig. 1 and Table 1).

To further explore how the subunit specificity of M3 governs the open duration we dissected M3 starting from the α1(M3ε) chimeric subunit, and we also introduced point mutations at key positions (Table 1). When only residues at positions 2′, 5′, 8′ and 10′ are replaced by their homologous in ε, the mean open time is prolonged with respect to wild-type channels but it is significantly briefer than that of α1(M3ε) (Table 1). The replacement of the first eleven residues of α1M3 by those found in εM3 increases the mean open time 13-fold with respect to wild-type, thus producing half of the effect α1(1′–11′M3ε) chimera, Table 1). Further replacement of residues 12′, 15′ and 20′ by those of ε does not lead to significant changes, indicating that these residues have little effect or that their individual effects are neutralized. Given that the chimera α1(1′–11′M3ε) carries mutations at 8′ and 9′, which have been previously shown to contribute to channel gating [15,16], we compared the changes with those produced by the single mutations at these positions. The exchange of α1F8′ in M3 by valine (α1F8′V), which is present in ε, increases slightly the mean open time with respect to wild-type AChRs (Table 1). However, α1V9′A mutant channels are 8-fold more prolonged. Thus, these two residues make

Table 1
M3 chimeric subunits

Chimera	M3																				τ_{on} (ms)
α1 subunit	1′								10′											20′	
α1(WT)	Y	M	L	F	T	M	V	F	V	I	A	S	I	I	I	T	V	I	V	I	N	0.90 ± 0.08
α1(M3ε)	Y	L	I	F	V	M	V	V	A	T	L	I	V	M	N	C	V	I	V	L	N	20.3 ± 3.6
α1(2′,5′,8′,10′M3ε)	Y	L	L	F	V	M	V	V	V	T	A	S	I	I	I	T	V	I	V	I	N	3.7 ± 0.7
α1(1′–11′M3ε)	Y	L	I	F	V	M	V	V	A	T	L	S	I	I	I	T	V	I	V	I	N	13.1 ± 1.4
α1(1′–11′+12′,15′,20′M3ε)	Y	L	I	F	V	M	V	V	A	T	L	I	I	I	N	T	V	I	V	L	N	14.9 ± 4.3
α1F8′V	Y	M	L	F	T	M	V	V	V	I	A	S	I	I	I	T	V	I	V	I	N	2.4 ± 0.4
α1V9′A	Y	M	L	F	T	M	V	F	A	I	A	S	I	I	I	T	V	I	V	I	N	8.8 ± 1.3
ε subunit																						
ε (WT)	Y	L	I	F	V	M	V	V	A	T	L	I	V	M	N	C	V	I	V	L	N	0.90 ± 0.08
ε (M3α1)	Y	M	L	F	T	M	V	F	V	I	A	S	I	I	I	T	V	I	V	I	N	0.17 ± 0.03
α1 subunit																						
α1(WT)	Y	M	L	F	T	M	V	F	V	I	A	S	I	I	I	T	V	I	V	I	N	0.90 ± 0.08
α1(1′–21′M3α7)	Y	F	A	S	T	M	I	I	V	G	L	S	V	V	V	T	V	I	V	L	R	0.29 ± 0.07
α1(1′–13′M3α7)	Y	F	A	S	T	M	I	I	V	G	L	S	V	I	I	T	V	I	V	I	N	0.49 ± 0.07
α1V7′I	Y	M	L	F	T	M	I	F	V	I	A	S	I	I	I	T	V	I	V	I	N	1.24 ± 0.10
α1F8′I	Y	M	L	F	T	M	V	I	V	I	A	S	I	I	I	T	V	I	V	I	N	1.75 ± 0.30

Alignment of M3 domains of α1, ε, and α7 subunits. α1 sequence is shown in white, ε in light grey, and α7 in dark grey. The right column shows the mean open time of the corresponding chimera. Values correspond to the mean and standard deviation of the duration of the slowest component of the open-time histogram for 3–6 patches per chimera.

the most significant contributions to the increase of open channel duration in the α1(1′–11′M3ε)-containing receptor.

To test if each partial chimera makes additive contributions to the closing rate, which was estimated by the inverse of the mean open time, we calculated the changes in the energy barrier for channel closing between different chimeric AChRs (Δ(ΔGc)). When ε sequence is placed in the whole segment of the α1 subunit (α1(M3ε)), the change in the energy for channel closing with respect to wild-type AChRs is 1.8 kcal/ mol. Δ(ΔGc) values calculated for the different partial chimeras with respect to the immediately shorter one are: 0.18 kcal/mol [between α1(M3ε) and α1(1′–11′+12′,15′,20′M3ε)]; 0.07 kcal/mol (between α1(1′–11′+12′,15′,20′M3ε) and α1(1′–11′M3ε); 0.73 kcal/mol (between α1(1′–11′M3ε) and α1(2′,5′,8′,10′M3ε); and 0.81 kcal/mol (between α1(2′,5′,8′,10′M3ε) and wild-type). The sum of the individual changes equals the change observed between the α1(M3ε) chimera and wild-type. This result confirms the additive contribution of each amino acid stretch of the M3 domain to channel closing rate.

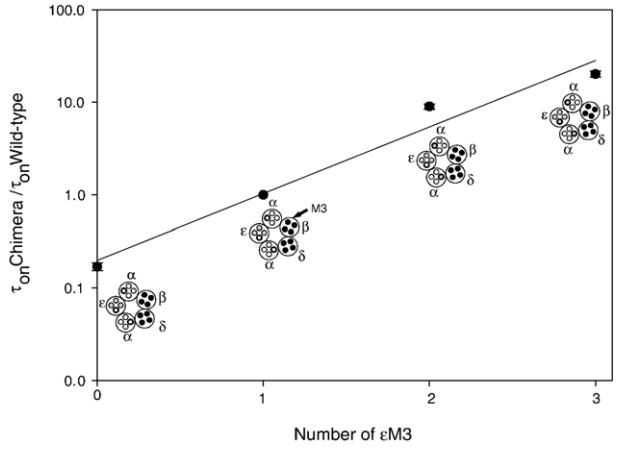

Fig. 2. Changes in the mean open time of chimeric AChRs as a function of the number of εM3 segments. Mean open times (τ_{on}) correspond to the slowest open component. Ratios plotted on a log scale display the data on a linear free energy scale. εM3=0 corresponds to AChRs containing the ε(M3α1) subunit; εM3=1 corresponds to wild-type; εM3=2 corresponds to α1(M3ε)+ε(M3α1); and εM3=3 corresponds to α1(M3ε). Values correspond to the mean±SD of at least four recordings for each chimera. Under each point, the schematic representation of the transmembrane segments of each chimeric AChR is shown. Colours are as in Fig. 1.

In the reverse chimera, in which M3 in the ε subunit is replaced by that of α1 (ε(M3α1)), changes in the mean open time opposite to those of the α1(M3ε) chimera are observed. Open-time histograms are well fitted by a single component whose duration is about 5-fold briefer than that of wild-type AChRs (Fig. 1 and Table 1).

The combination of α1(M3ε) and ε(M3α1) leads to intermediate mean open times. The receptor containing both chimeric subunits shows bursts composed of prolonged openings (τ_{on}= 9.05±0.95 ms) as well as isolated brief openings (τ_{on}=0.12± 0.03 ms), which result in two well distinguished components in the open-time histogram. We co-transfected cells with wild-type and chimeric subunits to construct AChRs containing a variable number of εM3 segments, ranging from 0 (which corresponds to AChRs containing the ε(M3α1) chimeric subunit) to 3 (which corresponds to receptors containing two α1(M3ε) subunits and wild-type ε). As shown in Fig. 2, the mean open time increases systematically with the increase in the number of εM3 segments. This result indicates that each εM3 segment makes additive contributions to the energy barrier of the closing process, increasing it by ~0.8 kcal/mol.

We next compared the functional changes conferred by the presence of mouse α7M3 in place of α1M3 (Fig. 1 and Table 1). Channel openings are 3-fold briefer than the control (Fig. 1). Further dissection shows that at least half of the reduction is

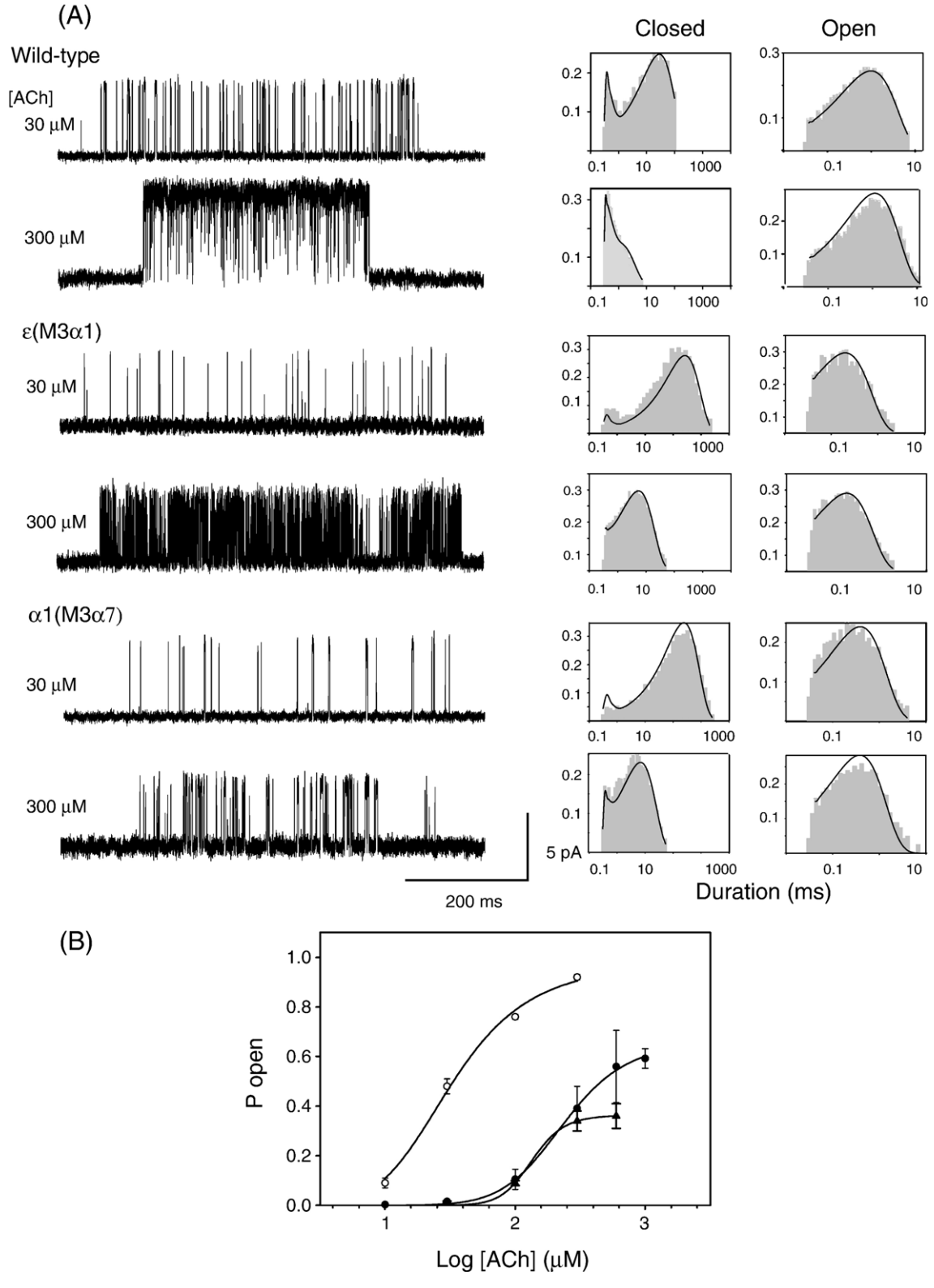

Fig. 3. Kinetics of activation of M3 chimeric AChRs. (A)—*Left*. Channel traces corresponding to wild-type AChRs or receptors containing the specified chimeric subunit activated by 30 and 300 μM ACh. Channels are displayed at a bandwidth of 9 kHz with openings as upward deflections. *Right*. Closed- and open-time histograms corresponding to the selected clusters with the fit for Scheme 1 superimposed. The ordinates correspond to the square root of the fraction of events per bin. (B)—Agonist-concentration dependence of the channel open probability for wild-type and chimeric AChRs. The mean fraction of time the channel is open during a cluster (P_{open}) was experimentally determined at the indicated concentrations of ACh. Each point corresponds to the mean ± SD of at least three patches. The symbols correspond to: ○ wild-type; ▲ ε(M3α1), and ● α1(M3α7) subunits.

Table 2
Kinetic parameters for wild-type and chimeric AChRs

AChR	k_{+1}	k_{-1}	k_{+2}	k_{-2}	β_1	α_1	β_2	α_2	k_{+b}	k_{-b}	θ_2
Wild-type	360±40	28,700±2500	180±20	57,400±5000	640±40	2600±140	50,000	1400±100	9±1	78,000	35.7
ε(M3α1)	190±10	42,000±2400	100±10	84,000±4300	nd	nd	19,700±600	6700±70	2	78,000	2.9
α1(M3α7)	250±20	40,500±3300	120±10	81,100±6600	nd	nd	8000±200	3000±50	6±1	78,000	2.7
α1F8′V	330±20	37,000±2300	160±10	74,000±4600	110±30	1550±390	50,000	600±20	3±1	78,000	83.3
α1V9′A	160±10	10,800±470	80±10	21,600±900	70±10	14,700±2300	50,000	180±10	6±1	78,000	277.8

Rate constants are in units of $\mu M^{-1}\ s^{-1}$ for the association rates and k_{+b} and s^{-1} for all others. θ_2 is the biliganded gating equilibrium constant (β_2/α_2). Values are results of a global fit to Scheme 1 of data obtained over a range of concentration of ACh, with error limits given as described in Materials and methods. ACh concentrations and number of different recordings used for the global fit were: For wild-type=10 μM (1), 30 μM (2), 100 μM (1) and 300 μM (2); for ε(M3α1)=30 μM (1), 100 μM (2), 300 μM (2) and 600 μM (1); and for α1(M3α7)=10 μM (1), 30 μM (2), 100 μM (2), 300 μM (1), 600 μM (1) and 1000 μM (1). For each condition more than 2000 events were included. Data not showing error have been constrained to allow a better fit. nd: not determined.

mediated by the first 13 amino acids of M3 (Table 1). The replacement of individual residues, such as those at positions 7′ and 8′ by the corresponding amino acids in α7, produces opposite effects to those originated by α1(M3α7), indicating that the final combination of residues is what governs channel closing.

3.3. Changes in activation kinetics of the chimeric AChRs

To determine unequivocally the kinetic step affected by the exchange of M3 between subunits we recorded single-channels at a range of desensitizing ACh concentrations (10–1000 μM). Very few channel openings from AChRs carrying the chimeric α1(M3ε) or the combination of α1(M3ε) and ε(M3α1) subunits are detected at ACh concentrations higher than 1 μM, and therefore kinetic analysis cannot be performed for these receptors. At agonist concentrations higher than 10 μM, wild-type AChRs open in clusters of episodes corresponding to a single AChR [36]. As shown in Fig. 3A, AChRs containing the chimeric ε(M3α1) or α1(M3α7) subunits show at all ACh concentrations clusters with briefer openings and prolonged intracluster closings compared to wild-type AChRs. We fitted the open- and closed-dwell times within clusters by the classical kinetic scheme (Scheme 1, [12]). In Scheme 1, two agonists (A) bind to receptors (R) in the resting state with association (k_{+1} and k_{+2}) and dissociation rates (k_{-1} and k_{-2}). AChRs occupied by one agonist open with rate β_1 and close with rate α_1, and AChRs occupied by two agonists open with rate β_2 and close with rate α_2. At high agonist concentrations channel block is evident and thus a block state, A_2R^* B, is included in the scheme.

Estimates of rate constants for wild-type AChRs are similar to those described before (Table 2, [12,13,26,27]). Monoliganded openings (AR* in Scheme 1) from AChRs carrying the chimeric subunits are not detected, and thus the data was best fitted by Scheme 1 lacking this state. The absence of this state in the model does not affect significantly the estimated rate constants of wild-type AChRs [26]. The scheme adequately describes the activation of AChRs containing ε(M3α1) or α1(M3α7) subunits (Fig. 3A). The results establish that the opening rate decreases 2-(ε(M3α1)) and 6-fold (α1(M3α7)), while the closing rate increases about 5-(ε(M3α1)) and 2-fold (α1(M3α7)). The channel gating equilibrium constant, $Z\theta_2$, calculated as β_2/α_2, decreases in both chimeric receptors (Table 2). Thus, these chimeric receptors open with greater latency, particularly if α7M3 is placed in the α1 subunit, and once opened they rapidly return to the closed state, particularly if α1M3 is placed in the ε subunit.

Although it was not possible to perform kinetic analysis for the α1(M3ε) chimeric receptor, we determined the kinetics of activation for AChRs containing the α1F8′V and α1V9′A mutations, which lead to changes in open durations. As shown in Table 2, the opening rate is not affected but the closing rate decreases 2- and 8-fold in α1F8′V and α1V9′A mutant AChRs, respectively. These changes correlate with the increase in the mean open time.

To evaluate overall functional changes in the ε(M3α1) and α1(M3α7) containing AChRs we determined the open probability in a range of ACh concentration (Fig. 3B). The curves for both chimeras are displaced to higher ACh concentrations owing to the impairment in channel gating. The EC_{50} values are 34 μM, 214 μM and 238 μM for wild-type, ε(M3α1), and α1(M3α7) respectively. In addition, the maximum P_{open} values are lower than that of wild-type AChR (Fig. 3B).

3.4. Subunit-selective contribution of M1 to channel gating

To determine if the subunit-selective contribution to open duration remains the same in the different transmembrane domains we replaced M1 in α1 by that of mouse ε and mouse α7 subunits (Table 3). The exchange of α1M1 by εM1 (α1(M1ε))

Table 3
M1 chimeric subunits

Chimera	M1																										τ_{on} (ms)
α1 subunit	1′									10′										20′							
α1(WT)	P	L	Y	F	I	V	N	V	I	I	P	C	L	L	F	S	F	L	T	S	L	V	F	Y	L	P	0.90 ± 0.08
α1(M1ε)	P	L	F	Y	V	I	N	I	I	V	P	C	V	L	I	S	G	L	V	L	L	A	Y	F	L	P	4.7 ± 1.2
α1(M1α7)	T	L	Y	Y	G	L	N	L	L	I	P	C	V	L	I	S	A	L	A	L	L	V	F	L	L	P	11.7 ± 1.7

Alignment of M1 domains of α1, ε and α7 subunits. α1 sequence is shown in white, ε in light grey, and α7 in dark grey. The right column shows the mean open times of the corresponding AChRs. Values correspond to the mean and SD of the duration of the slowest component of the open-time histogram for 3 to 6 patches per chimera.

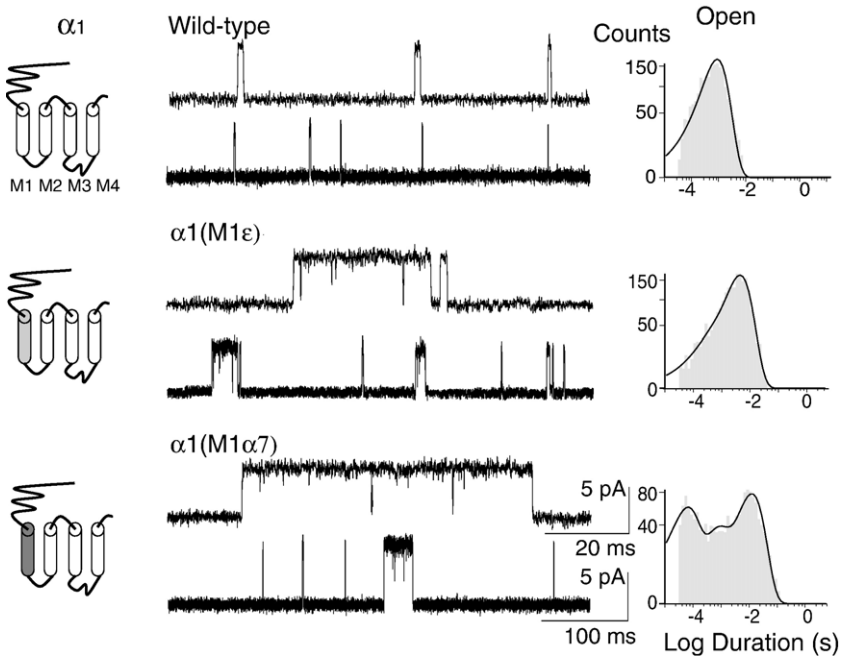

Fig. 4. Single-channel recordings of wild-type and M1 chimeric AChRs. *Left*. Schematic representation of chimeric α1 subunits. Light grey corresponds to ε sequence and dark grey to α7. *Right*. Channels activated by 1 μM ACh. Currents are displayed at a bandwidth of 9 kHz with channel openings as upward deflections. Membrane potential: −70 mV. Open-time histograms of AChRs carrying the specified chimeric subunit are shown. The mean durations and relative areas of the open components in the histograms are: wild-type = 0.96 ms (0.85) and 0.21 ms; α1(M1ε) = 5.15 ms (0.88) and 0.36 ms; α1(M1α7) = 11.76 ms (0.58), 0.96 ms (0.29) and 0.25 ms.

produces qualitatively similar changes in the mean open time to those observed in the M3 chimera although channel openings are not so prolonged. AChRs carrying the chimeric α1(M1ε) subunit also show activation in bursts at 1 μM ACh and two open components (Fig. 4 and Table 3). In contrast, the chimeric α1 (M1α7) AChR shows a completely different behavior from that of receptors containing the α1(M3α7) subunit. Activation of this receptor appears in bursts of very long openings at low ACh concentrations (Fig. 4 and Table 3). In addition to these long openings, it also shows two classes of brief isolated openings (τ_{on} = 1.3 ± 0.7 and 0.22 ± 0.05 ms), which results in three well distinguished components in the open-time histogram (Fig. 4). Recordings performed at different ACh concentrations show that the relative area of the slowest open component increases as a function of ACh concentration. The relative areas are 0.32 ± 0.07 at 50 nM ACh and 0.63 ± 0.06 at 1 μM ACh ($p < 0.001$). This observation suggests that the slowest open component may correspond to biliganded AChRs. Three open components have been shown for other mutant AChRs, such as the one carrying a mutation in M1 (εL221F) that is associated with a slow-channel myasthenic syndrome [37]. The two briefest components were proposed to correspond to monoliganded AChRs [37].

Taken together, our results reveal that each transmembrane domain contributes in a unique way to AChR activation kinetics and that the structural bases of the subunit selectivity are different in the transmembrane domains.

4. Discussion

This work reveals that each M3 transmembrane domain contributes to channel gating as a whole in a subunit-selective manner and that its contribution is additive among subunits and composing residues. M3 chimeric subunits are incorporated into functional channels. However, a reduction in AChR expression takes place. AChR channel assembly and expression are complex processes and the precise mechanisms involved are still unknown [33,38]. The reduced surface expression of the chimeric AChRs suggests that the changes in M3 may affect some of the steps by which newly synthesized subunits are transformed into surface functional AChRs. Effects of mutations in M3 on assembly and/or oligomerization have been suggested before [18].

The decay rates of ACh-activated currents from M3 chimeric AChRs are similar to that of wild-type currents. These results show that the changes in M3 sequence do not affect the desensitization rate from the open state although they affect significantly the single-channel properties.

Single-channel recordings reveal that the exchange of M3 between subunits affects gating kinetics. The most significant change occurs when M3 of α1 is replaced by that of ε. This could be due to the fact that the ε subunit had a relative late appearance during evolution and the amino acid identity between α1 and ε subunits is low, only 30% in human subunits [39]. Interestingly, the reverse chimera in which M3 of the ε subunit is replaced by that of α1 leads to opposite behavior: activation of ε(M3α1)-containing AChR is clearly impaired, and channels show briefer durations and prolonged intracluster closings with respect to wild-type AChRs. Kinetic analysis revealed that these changes are due to a reduction in the opening rate and an increase in the closing rate.

Increasing the number of M3 domains containing α1 sequence leads to progressively larger decreases in the duration

of the open state. Thus, each M3 segment makes additive contributions to the energy barrier of closing. These results agree with our previous studies showing that position 8′ of M3 of all subunits contribute additively to channel gating [16].

A recent study revealed that α1M3 adopts two different helical structures: a thinner-elongated helix in the closed state and a thicker-shrunken in the open state, thus suggesting that it undergoes conformational changes during gating [18]. In agreement with this, the subunit-selective contribution to gating could be due to the structural differences which may affect the conformational helical changes that accompany channel gating.

To compare the functional changes between chimeric receptors we evaluated the duration of the mean open time and estimated the closing rate as the inverse of the mean open time. Changes in apparent mean open time could be due to changes in rate constants underlying either ACh binding or channel gating steps. However, several studies have shown that mutations in M3 mainly affect the closing rate and do not produce significant changes in the agonist-dissociation rate [15,16,19]. In agreement with this, only slight changes in the dissociation rates are observed in ε(M3α1) and α1(M3α7) chimeric AChRs. Moreover, the increase in the closing rate of these receptors (4.8-fold for ε(M3α1) and 2-fold for α1(M3α7)) determined by kinetic analysis correlates with the decrease in the mean open time (5.2-fold and 3-fold for ε(M3α1) and α1(M3α7), respectively).

Dissection of M3 shows that the contributions to the open duration of its composing residues are additive. Mutations at individual residues may not affect or may affect in opposite manners the closing rate, leading to gain or loss of function, but when combined together, the final effect will result from the addition of the individual effects. Moreover, the dissection of the α1(M3ε) chimera confirms this result as the changes in the energy barrier for channel closing are additive when different stretches of M3 are considered. This suggests that the overall conformation, which in turn is given by the amino acid sequence, is the main determinant of gating kinetics. This observation agrees with the rate–equilibrium linear free energy study which shows a Φ value of 0.3 for all residues at the upper half of the M3 helix, suggesting that they move in block [19].

Mutation at position 9′ of the α1 subunit (V285I) has been found to be the cause of the attenuated postsynaptic response observed in a patient suffering from a congenital myasthenic syndrome [15]. The present results confirm the significant functional role of this residue as it is responsible for a great proportion of the increase in channel open time observed in the α1 (1′–11′M3ε) chimera.

The analysis of α1M1 chimeric AChRs reveals that also M1 contributes to channel gating in a subunit-selective manner although the structural bases of the subunit selectivity is differently conserved among transmembrane domains. For example the replacement of α1M1 by α7 leads to gain of function whereas it produces loss of function in M3. Interestingly, muscle AChRs containing α7M3 shows briefer channels, which resemble α7 channels [40,41]. However when α7M1 is placed instead of α1M1, channel duration is prolonged, showing that the closing rate is a complex controlled process. It is interesting to note that although the open duration is increased in α1 (M1α7), α1(M1ε) and α1(M3ε) chimeric receptors, the open-time histograms are completely different, showing two (α1 (M3ε) and α1(M1ε)) or three (α1(M1α7)) open components. Therefore, the molecular mechanisms underlying the functional changes are specific for each transmembrane domain and subunit.

In summary, multiple functionally distinct AChRs result from the assembly of different subunits. Each subunit provides special structural features which, when combined in the whole AChR, have a functional significance. Our results support the importance of the subunit-selective contribution of M3 to channel activation.

Acknowledgments

This work was supported by grants from CONICET, Universidad Nacional del Sur, FONCYT and a fellowship from John Simon Guggenheim Memorial Foundation to CB.

References

[1] N. Le Novere, J.P. Changeux, Molecular evolution of the nicotinic acetylcholine receptor: an example of multigene family in excitable cells, J. Mol. Evol. 40 (1995) 155–172.
[2] J.L. Galzi, A. Devillers-Thiery, N. Hussy, S. Bertrand, J.P. Changeux, D. Bertrand, Mutations in the channel domain of a neuronal nicotinic receptor convert ion selectivity from cationic to anionic, Nature 359 (1992) 500–505.
[3] M.H. Akabas, C. Kaufmann, P. Archdeacon, A. Karlin, Identification of acetylcholine receptor channel-lining residues in the entire M2 segment of the alpha subunit, Neuron 13 (1994) 919–927.
[4] A. Miyazawa, Y. Fujiyoshi, N. Unwin, Structure and gating mechanism of the acetylcholine receptor pore, Nature 424 (2003) 949–955.
[5] H.A. Lester, M.I. Dibas, D.S. Dahan, J.F. La Diba, D.S. Midan, J.F. Leite, D.A. Dougherty, Cys-loop receptors: new twists and turns, Trends Neurosci. 27 (2004) 329–336.
[6] N. Unwin, Refined structure of the nicotinic acetylcholine receptor at 4 Å resolution, J. Mol. Biol. 346 (2005) 967–989.
[7] P. Purohit, A. Mitra, A. Auerbach, A stepwise mechanism for acetylcholine receptor channel gating, Nature 446 (2007) 930–933.
[8] H.L. Wang, A. Auerbach, N. Bren, K. Ohno, A.G. Engel, S.M. Sine, Mutation in the M1 domain of the acetylcholine receptor alpha subunit decreases the rate of agonist dissociation, J. Gen. Physiol. 109 (1997) 757–766.
[9] G. Spitzmaul, J. Corradi, C. Bouzat, Mechanistic contributions of residues in the M1 transmembrane domain of the nicotinic receptor to channel gating, Mol. Membr. Biol. 21 (2004) 39–50.
[10] S. Tamamizu, Y. Lee, B. Hung, M.G. McNamee, J.A. Lasalde-Dominicci, Alteration in ion channel function of mouse nicotinic acetylcholine receptor by mutations in the M4 transmembrane domain, J. Membr. Biol. 170 (1999) 157–164.
[11] S. Tamamizu, G.R. Guzmán, J. Santiago, L.V. Rojas, M.G. McNamee, J.A. Lasalde Dominicci, Functional effects of periodic tryptophan substitutions in the alpha M4 transmembrane domain of the *Torpedo californica* nicotinic acetylcholine receptor, Biochemistry 39 (2000) 4666–4673.
[12] C. Bouzat, F. Barrantes, S. Sine, Nicotinic receptor fourth transmembrane domain: hydrogen bonding by conserved threonine contributes to channel gating kinetics, J. Gen. Physiol. 115 (2000) 663–672.
[13] C. Bouzat, F. Gumilar, M.C. Esandi, S.M. Sine, Subunit-selective contribution to channel gating of the M4 domain of the nicotinic receptor, Biophys. J. 82 (2002) 1920–1929.
[14] A. Mitra, T.D. Bailey, A.L. Auerbach, Structural dynamics of the M4 transmembrane segment during acetylcholine receptor gating, Structure 12 (2004) 1909–1918.

[15] H.L. Wang, M. Milone, K. Ohno, X.M. Shen, A. Tsujino, A.P. Batocchi, P. Tonali, J. Brengman, A.G. Engel, S.M. Sine, Acetylcholine receptor M3 domain: stereochemical and volume contributions to channel gating, Nat. Neurosci. 2 (1999) 226–233.
[16] M.J. De Rosa, D. Rayes, G. Spitzmaul, C. Bouzat, Nicotinic receptor M3 transmembrane domain: position 8′ contributes to channel gating, Mol. Pharmacol. 62 (2002) 406–414.
[17] M. Navedo, M. Nieves, L. Rojas, J.A. Lasalde-Dominicci, Tryptophan substitutions reveal the role of nicotinic acetylcholine receptor alpha-TM3 domain in channel gating: differences between *Torpedo* and muscle-type AChR, Biochemistry 43 (2004) 78–84.
[18] J.D. Otero-Cruz, C.A. Baez-Pagan, I.M. Caraballo-Ganzalez, J.A. Lasalde-Dominicci, Tryptophan-scanning mutagenesis in the alphaM3 transmembrane domain of the muscle-type acetylcholine receptor. A spring model revealed, J. Biol. Chem. 282 (2007) 9162–9171.
[19] D.J. Cadugan, A. Auerbach, Conformational dynamics of the αM3 transmembrane helix during acetylcholine receptor-channel gating, Biophys. J. 93 (2007) 859–865.
[20] C. Bouzat, N. Bren, S.M. Sine, Structural basis of the different gating kinetics of fetal and adult acetylcholine receptors, Neuron 13 (1994) 1395–1402.
[21] C. Bouzat, A.M. Roccamo, I. Garbus, F.J. Barrantes, Mutations at lipid-exposed residues of the acetylcholine receptor affect its gating kinetics, Mol. Pharmacol. 54 (1998) 146–153.
[22] O.P. Hamill, A. Marty, E. Neher, B. Sakmann, F.J. Sigworth, Improved patch-clamp techniques for high-resolution current recording from cells and cell-free membrane patches, Pflugers Arch. 391 (1981) 85–100.
[23] F. Qin, A. Auerbach, F. Sachs, Estimating single-channel kinetic parameters from idealized patch-clamp data containing missed events, Biophys. J. 70 (1996) 264–280.
[24] C. Grosman, A. Auerbach, Asymmetric and independent contribution of the second transmembrane segment 12′ residues to diliganded gating of acetylcholine receptor channels: a single-channel study with choline as the agonist, J. Gen. Physiol. 115 (2000) 637–651.
[25] S.M. Sine, K. Ohno, C. Bouzat, A. Auerbach, M. Milone, J.N. Pruitt, A.G. Engel, Mutation of the acetylcholine receptor alpha subunit causes a slow-channel myasthenic syndrome by enhancing agonist binding affinity, Neuron 15 (1995) 229–239.
[26] F.N. Salamone, M. Zhou, A. Auerbach, A re-examination of adult mouse nicotinic acetylcholine receptor channel activation kinetics, J. Physiol. 516 (1999) 315–330.
[27] G. Akk, A. Auerbach, Inorganic, monovalent cations compete with agonists for the transmitter binding site of nicotinic acetylcholine receptors, Biophys. J. 70 (1996) 2652–2658.
[28] G. Spitzmaul, J.P. Dilger, C. Bouzat, The noncompetitive inhibitor quinacrine modifies the desensitization kinetics of muscle acetylcholine receptors, Mol. Pharmacol. 60 (2001) 235–243.
[29] F. Gumilar, H.R. Arias, G. Spitzmaul, C. Bouzat, Molecular mechanisms of inhibition of nicotinic acetylcholine receptors by tricyclic antidepressants, Neuropharmacology 45 (2003) 964–976.
[30] K. Brejc, W.J. van Dijk, R.V. Klaassen, M. Schuurmans, J. van Der Oost, A.B. Smit, T.K. Sixma, Crystal structure of an ACh-binding protein reveals the ligand-binding domain of nicotinic receptors, Nature 411 (2001) 269–276.
[31] X.M. Yu, Z.W. Hall, Extracellular domains mediating epsilon subunit interactions of muscle acetylcholine receptor, Nature 352 (1991) 64–67.
[32] K. Sumikawa, V.M. Gehle, Assembly of mutant subunits of the nicotinic acetylcholine receptor lacking the conserved disulfide loop structure, J. Biol. Chem. 267 (1992) 6286–6290.
[33] W.N. Green, Ion channel assembly: creating structures that function, J. Gen. Physiol. 113 (1999) 163–170.
[34] N.S. Millar, Assembly and subunit diversity of nicotinic acetylcholine receptors, Biochem. Soc. Trans. 31 (2003) 869–874.
[35] S.M. Sine, T. Claudio, F.J. Sigworth, Activation of *Torpedo* acetylcholine receptors expressed in mouse fibroblasts. Single channel current kinetics reveal distinct agonist binding affinities, J. Gen. Physiol. 96 (1990) 395–437.
[36] B. Sakmann, J. Patlak, E. Neher, Single acetylcholine-activated channels show burst-kinetics in presence of desensitizing concentrations of agonist, Nature 286 (1980) 71–73.
[37] C.J. Hatton, C. Shelley, M. Brydson, D. Beeson, D. Colquhoun, Properties of the human muscle nicotinic receptor, and of the slow-channel myasthenic syndrome mutant epsilonL221F, inferred from maximum likelihood fits, J. Physiol. 547 (2003) 729–760.
[38] C.P. Wanamaker, W.N. Green, ER chaperones stabilize nicotinic receptor subunits and regulate receptor assembly, J. Biol. Chem. 282 (2007) 31113–31123.
[39] M.O. Ortells, G.G. Lunt, Evolutionary history of the ligand-gated ion-channel superfamily of receptors, Trends Neurosci. 18 (1995) 121–127.
[40] A. Mike, N.G. Castro, E.X. Albuquerque, Choline and acetylcholine have similar kinetic properties of activation and desensitization on the alpha7 nicotinic receptors in rat hippocampal neurons, Brain Res. 882 (2000) 155–168.
[41] A.N. Placzek, F. Grassi, E.M. Meyer, R.L. Papke, An alpha7 nicotinic acetylcholine receptor gain-of-function mutant that retains pharmacological fidelity, Mol. Pharmacol. 68 (2005) 1863–1876.